DECEMBER 14 2023

Corrected frequency-dependent directivity indices for large solid rocket motors FREE

Grant W. Hart ; Kent L. Gee ; Mylan R. Cook

Proc. Mtgs. Acoust. 51, 040007 (2023)
https://doi.org/10.1121/2.0001810

Volume 51 http://acousticalsociety.org/

184th Meeting of the Acoustical Society of America
Chicago, Illinois
8-12 May 2023

Noise: Paper 1aNS3

Corrected frequency-dependent directivity indices for large solid rocket motors

Grant W. Hart, Kent L. Gee and Mylan R. Cook
Department of Physics and Astronomy, Brigham Young University, Provo, UT, 84602; grant_hart@byu.edu; kentgee@byu.edu; mylan.cook@gmail.com

For many years, empirical models for rocket noise radiation relied on the directivity indices published in NASA SP-8072 (K. Eldred, 1971). Because these were known to have inaccuracies, NASA led a project to update the indices using a Space Shuttle reusable solid rocket motor (RSRM). The RSRM measurements, involving an angular arc at a radius of about 80 nozzle exit diameters, centered on the nozzle, resulted in updated directivity indices (Haynes and Kenny, AIAA 2009-3160). However, the source position is not at the nozzle, so James et al. (Proc. Mtgs. Acoust., 18, 040008, (2012)) corrected the low-frequency indices using an estimated dominant source position for each frequency. That paper was an improvement, but later measurements have shown that it also had some nonphysical results. This paper revisits that correction by using near-field vector intensity measurements from a similar, but smaller, GEM-60 motor to determine the frequency-dependent source position to adjust the apparent angles and distances of the measurements. Additionally, an effort is made to account for plume impingement downstream that likely resulted in lower high-frequency levels than would have been measured otherwise. This analysis results in updated, frequency dependent directivity indices for a large solid rocket motor.

Published by the Acoustical Society of America

 https://doi.org/10.1121/2.0001810

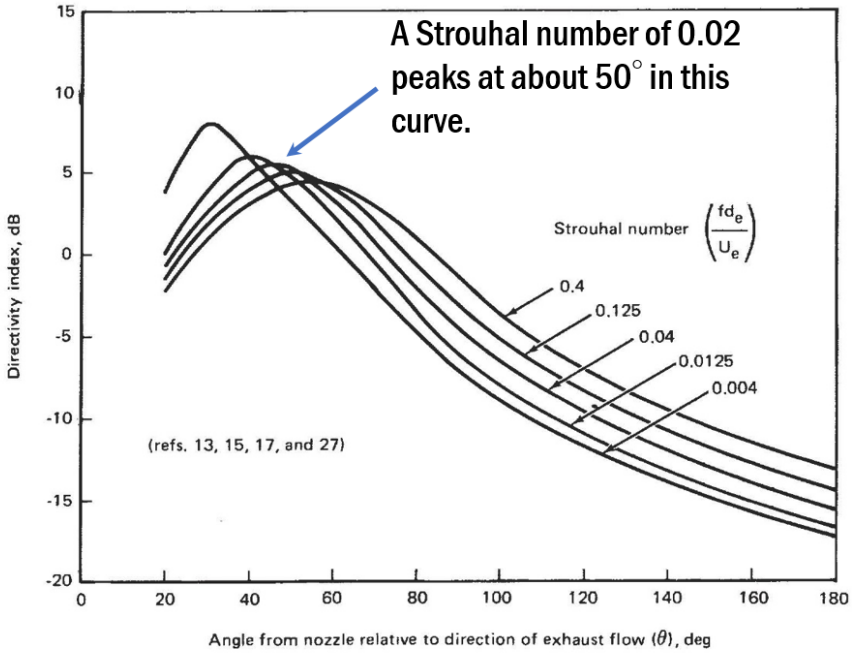

Figure 1: The directivities published in NASA's report SP-8072. These are known to be flawed. For example the peak directivity for a Strouhal number of 0.02 (typical of rockets) occurs at an angle of about 50° from the direction of the plume in these curves. Experimentally it is found to be much closer to 65-70°. Figure modified from NASA SP-8072[1]

1. INTRODUCTION

The noise emitted from a rocket as it is launched is highly directional, so anyone modeling rocket noise needs to have information about how the radiated power is spatially distributed. This is done by using the directivity index. The directivity index of a rocket is the far-field sound pressure level of the sound as a function of angle, relative to a monopole source of the same total power. The directivity index is a function of both frequency and angle.

During the space-race era, NASA published a report (usually referred to as SP-8072[1]) that characterized the sound produced by chemical rockets, as it was then understood. This included a set of directivity indices for the noise, as shown in Figure 1. This figure shows a number of curves of the radiation relative to a monopole, in decibels, as a function of angle relative to the plume of the rocket. The curves are parameterized by Strouhal number, which is the frequency times the nozzle diameter divided by the velocity of the gas in the plume as it exits the nozzle ($Sr = fD/v$). The Strouhal number defined this way appears to scale different size rockets to roughly the same set of curves.

Research during the last 50 years has shown that these indices were flawed. For example, a typical liquid-fueled rocket has a Strouhal number in the vicinity of 0.02. According to Figure 1, this should have a peak radiation power at about 50°. However, measurements made in the far field of launched rockets[2–4] show peak directivity at closer to 65-70°.

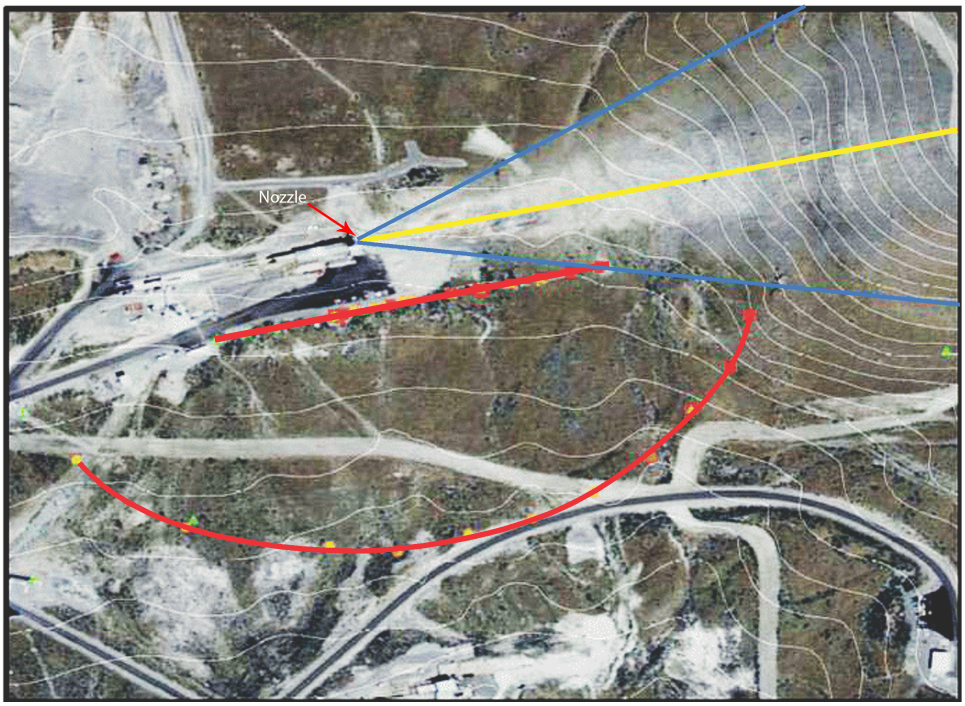

Figure 2: The layout of the NASA RSRM project. The blue lines show the plume boundary. The red lines show the positions of the microphone around the nozzle The yellow line shows the direction of the plume. The light lines are elevation contours at 5 m intervals. The arc has a radius of approximately 80 nozzle diameters centered on the nozzle. Figure derived from Pilkey and Kenny (2011)[6]

2. NASA'S RSRM MEASUREMENTS

In the late 2000s NASA led a project to update those indices using the Reusable Solid Rocket Motor (RSRM), which was used for the Space Shuttle program.[5,7] The RSRM had a thrust typical of modern heavy-lift rockets, and so the measurements would not have to be extrapolations from the smaller rockets used to produce SP-8072. The RSRM measurements were made during three static firings of the RSRM at Promontory, UT, at the test facility of ATK Space Systems, the manufacturer of the motor.

The layout of these measurements is shown in Figure 2. The RSRM is the black line in the upper-left quadrant. The direction of the plume is shown by the yellow line, with the impact area of the plume outlined with the blue lines. This is the plume width plus additional space to allow the nozzle to gimbal during the test. The microphones were placed along the lines indicated in red in the figure. One set was near to, and parallel to, the plume and booster. The second set was placed along an arc at a radius of approximately 80 nozzle diameters, with the arc centered on the rocket's exit nozzle. The microphones were separated by 10° on the arc. The light white lines in the figure are elevation contour lines with 5 m spacing. As can be seen in the figure the plume impinges on the hill near the position of the last two microphones (on the right) on the arc.

A. CHALLENGES INTERPRETING THE MEASUREMENT

The simplest interpretation of the data is to assume that the source is a compact source located at the nozzle. Then the directivity can be directly derived from the angular position of the microphones relative to the nozzle, as was done in Haynes, et al.[7] This is illustrated in part (A) of Figure 3. The challenges with this are twofold. First, the source of the noise from a supersonic jet is now known to be located many

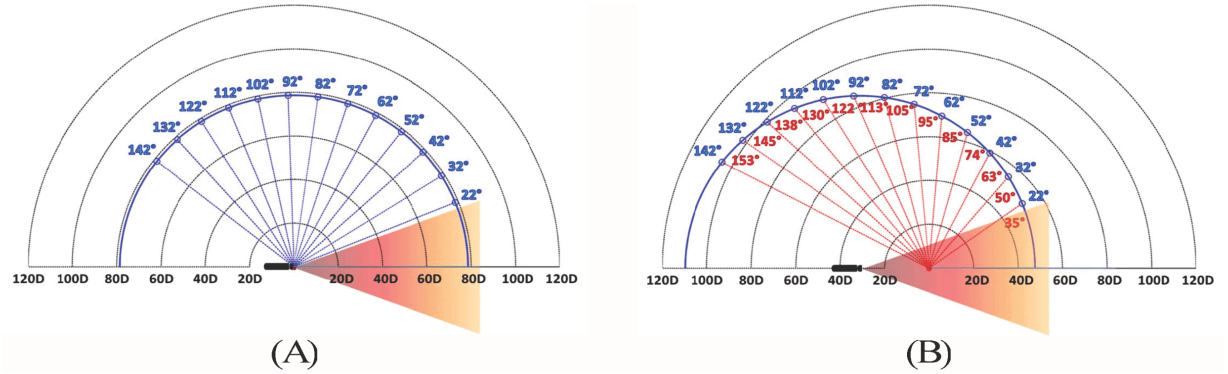

Figure 3: Part (A) shows the layout of the NASA measurement microphones on the arc relative to the the nozzle. They were spaced 10° apart, from 22° to 142°, at a radius of 80 nozzle diameters. If the sound source is downstream from the nozzle, both the angle of the radiated sound and distance to the microphone is different. This figure shows the corrected angles and distances for a source about 33 D downstream of the nozzle. Figures reproduced from James et al.,[8] with permission of Acoustical Society of America. Copyright 2012, Acoustical Society of America.

nozzle diameters downstream. This means that, especially for lower frequencies, the microphones are not in the far field,[8] which means that the angles between the noise source and the microphones are not the same as previously assumed. Part (B) of Figure 3 the distances and angles of the microphones where the sound source is 33 nozzle diameters downstream. Clearly this can be a significant adjustment.

The correction needs to be made, not only for the geometrical angle, but the SPL needs to be corrected for spherical spreading to put the measurements at a corrected common distance. Another aspect of this problem is that the sound source position depends on frequency, and so the correction to the directivity indices differs as a function of frequency.

Another challenge with this dataset has to do with the impingement of the plume on the hillside. This appears to have affected some of the data, as will be discussed in a later section.

3. CORRECTION OF THE INDICES

Both of these problems were recognized a few years after the RSRM data were published,[8,9] and an attempt was made to correct the sound source position problem.

A. PREVIOUS ATTEMPT TO CORRECT THIS DATA

The key to the correction is knowing the position the sound source as a function of frequency. Unfortunately, there was not an accurate way to determine the source location with the setup of the measurement. However, an attempt was made to correct the data using the linear array of microphones that was parallel to the plume.[8] The sound source was assumed to be at the location on the close linear array where sound at that frequency was the loudest. This would be a reasonably good assumption if the source were a monopole, but since the sound from a rocket plume is very directional, the assumption breaks down.

The derived curve of axial position of the source vs. Strouhal number is shown as the blue curve on Figure 6. This curve is nonphysical, particularly at high frequencies where the source is presumed to be right at the nozzle. The physics of noise production from a jet doesn't allow the noise to originate at this location. It takes time (and distance) for the turbulence to develop into a source.

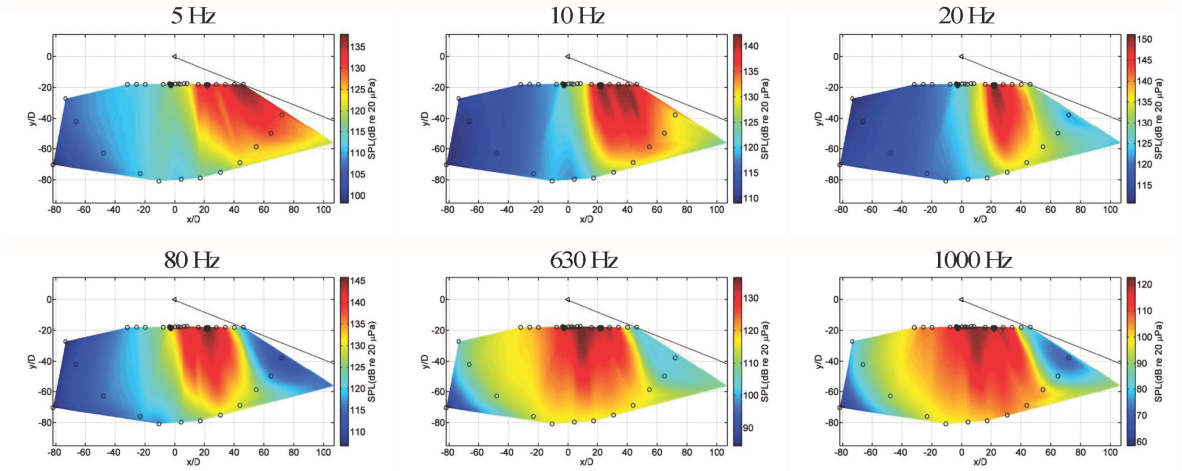

Figure 4: Interpolated SPL maps of the data from the RSRM firing. Starting at about 20 Hz and getting progressively worse as the frequency goes up, there is an unphysical cutoff in the data at small angles (on the right side of the figure. Reproduced from Gee et al.[9] with permission of Acoustical Society of America. Copyright 2012, Acoustical Society of America.

The method used to correct the indices was to geometrically calculate both the new angle and the new distance for a microphone relative to the assumed sound source position, as shown in Figure 3 part (B). The level for that microphone was then put at the new angle and the SPL was adjusted from whatever its new distance was to a common distance, assuming spherical spreading. They used 80 nozzle diameters, since that was where the original array was supposed to be located. This correction method was valid, but the frequency-dependent source location needed improvement.

B. THE EFFECT OF IMPINGEMENT

Figure 4 shows interpolated maps of the SPL from the measurement.[9] As can be seen in the plots there is a cutoff in the data at small angles (on the right side of the figure) starting at about 20 Hz and getting worse as the frequency goes up. This cutoff is unphysical for a free plume. It is interesting to note that the plume starts to impinge on the hillside near the location where this cutoff occurs. Gee et al.[9] also noted that when the nozzle was vectored upward from the ground some of the effects of impingement were reduced. No attempt to correct for this effect was made previously.

4. CORRECTION OF THE DATA

The purpose of the current study was to improve the directivity indices by correcting both of these problems.

A. IMPINGEMENT CORRECTION

Looking at the data in Figure 7, we can see that all the frequencies have a roughly linear decrease in directivity index from 42° to 22°. It is apparent when looking at the data shown in Figure 4, that the lowest-frequency data is affected by the impingement the least. It therefore seems reasonable to replace all the

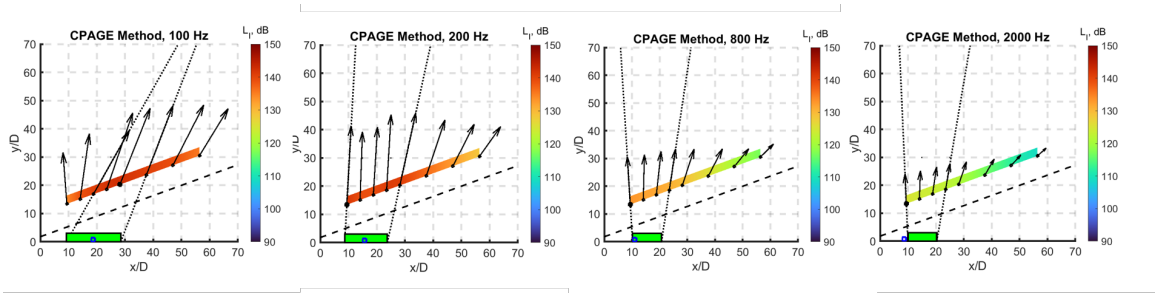

Figure 5: Intensity probe results from a GEM-60 static firing. The arrows shown are the intensity vectors measured at each probe location. They are plotted as the one-fourth-power of the actual intensity to keep them visible on the page. The green bar at the bottom is the region that the appears as sources for the 3-dB down region of the intensity. The dot shows the position of the source for the peak intensity. Note that the source moves toward the nozzle as the frequency increases.

higher frequency curves between 42° and 22° with linear segments with the same slope as the 10 Hz curve, assuming that without the impingement the curves would fall off at about the same rate.

B. SOURCE LOCATION USING INTENSITY DATA

The next task is to locate the source position. Unfortunately, there is no data set that shows the intensity of the sound emitted from the RSRM, which is necessary to trace the radiated sound back to the sound source. However, we have intensity data[10] from the firing of a similar, but smaller, rocket (a GEM-60), along a line near the plume.

This data set consists of eight 2” radius 2-D intensity probes, positioned along a line parallel to the outer edge of the plume. The closest probe to the nozzle was about 10 nozzle diameters downstream. It could not be located any closer to the nozzle because of a pillar in the testing facility. The probes were located about 6-7 diameters apart along this line.

Using the CPAGE method[12] to determine the direction and intensity from the data at each probe produces the results shown in Figure 5. In each of these plots the frequency is shown in the title at the top of the plot. The vectors lengths shown are the fourth-root of the magnitude of the intensity. This was done so that the vectors of all the probes can be seen on the same plot. The two long lines represent the vectors along the lines from the probes that are 3 dB down from the peak intensity. Those are traced back to define a source region. Note that at 100 Hz the system is running into the limitations of the 2” radius probe, even with the CPAGE method, producing vector directions that are not reliable. The estimated source region is shown by a green box along the x-axis. The dot shown is estimated peak of the source region, obtained by fitting the source strength along the axis and finding the peak.

At higher frequencies this peak is shown to the left of the source region. That is because of the limits imposed by the closest probe being 10 diameters away from the nozzle.

The data of source position versus Strouhal number from this measurement can be fit to a power law of the form

$$\frac{x}{D} = ASr^B \tag{1}$$

and produces the green curve that is shown in Figure 6. The distances range from about 7 nozzle diameters away at high frequencies to about 50 diameters at the lowest frequencies. The red curve in Figure 6 is derived from the same dataset used here,[10] but the analysis method was not as robust and so couldn’t locate the high-frequency source as well, given that the closest probes were 10D downstream.

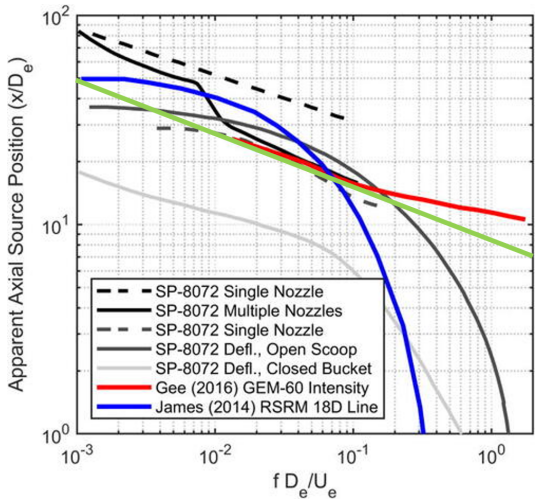

Figure 6: Source position as a function of Strouhal number. Adapted from Lubert, et al. (2022). The green line is our estimate taken from the intensity data on a GEM-60 static firing. Adapted from Lubert, et al.,[11] with permission of Acoustical Society of America. Copyright 2022, Acoustical Society of America.

5. RESULTS

Figure 7 shows the original directivity indices from Kenny et al.[5] as well as a colormap extrapolated beyond the measured angles from 0° to 180°. Note the deep hole in the lower-right corner of the plot, caused by the impingement of the plume and the unphysical peak of the directivity index at 40° for 10 Hz.

Figure 8 shows the effect of both corrections applied to the data. The directivity indices are shown on the left and the colormap is on the right. Note the increase in the peak directivity index at the lowest frequencies, as well as the removal of the unphysical hole in the data at higher frequencies and low angles.

Figure 9 shows a colormap of the difference between the original data and the corrected data. The most significant differences are at low frequencies and moderate angles, and again at high frequencies and low angles.

A. PROPERTIES OF THE PEAKS

Figure 10 shows the properties of the directivity index peaks. The curves in part (A) show the positions of both the original peaks and the modified peaks. The correction moved the peaks to higher angles, more in accordance with recent measurements. Part (B) shows the width of the peaks, defined as the distance between the 3-dB down points of the directivity index curve. The correction widened all but the highest frequencies. It is interesting to note that the highest frequencies appear to have similar angles and widths as the lowest frequencies. This might be an indication that what we are seeing in this spectral region is not a result of the intrinsic properties of the source, but rather a result of atmospheric absorption of the sound produced by the source, along with nonlinear propagation and shock formation creating new high-frequency content by the time the sound has propagated to the microphones.

6. CONCLUSIONS

In conclusion, the analysis of the measured directivity indices of the static-fired RSRM boosters was improved in two ways. First, the high frequency energy lost due to the plume impingement on the hillside was estimated and put back into the indices. Second, the error made by assuming that the sound source was at the nozzle of the rocket was corrected for.

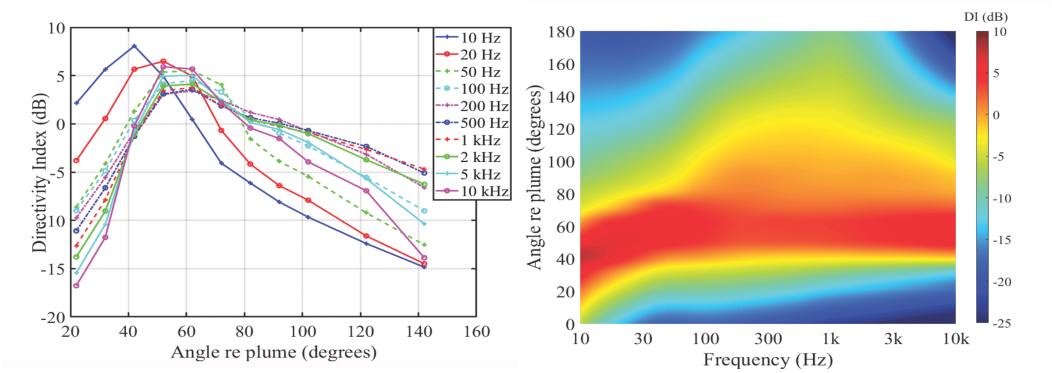

Figure 7: Plots showing the original directivity indices on the left at specified frequencies and a colormap on the right showing an interpolated colormap of the same data.

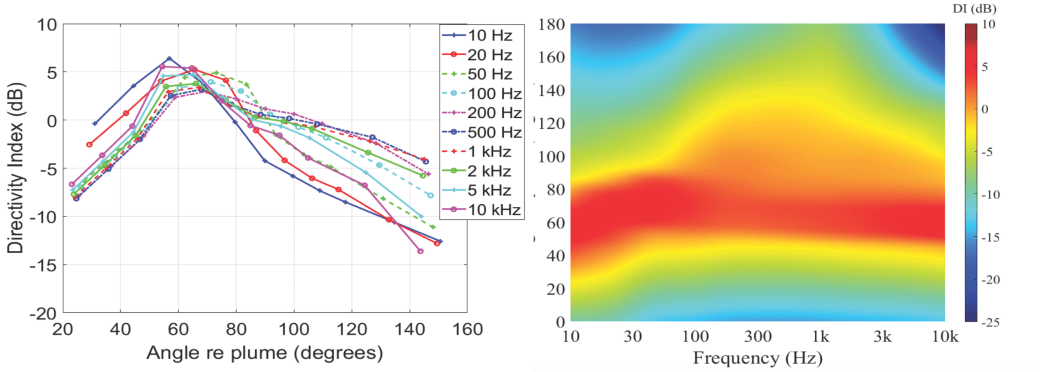

Figure 8: Plots showing the directivity indices with all corrections applied. On the left the data are plotted at specified frequencies and the colormap on the right shows an interpolated colormap of the same data set. Note upward shift in peak frequency on the left-hand side of this plot compared to the previous plot, as well as the elimination of the abnormally low levels in the lower-right-hand corner.

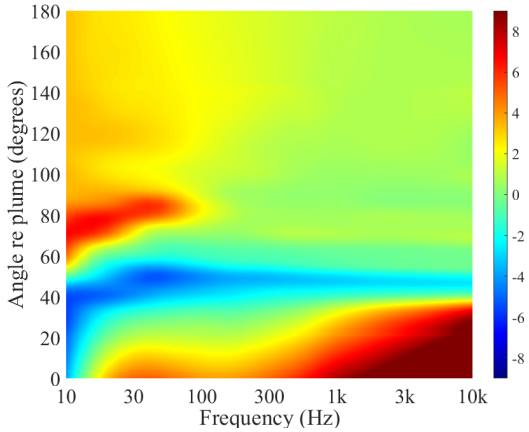

Figure 9: The difference between the corrected data and the original NASA directivity indices, in decibels.

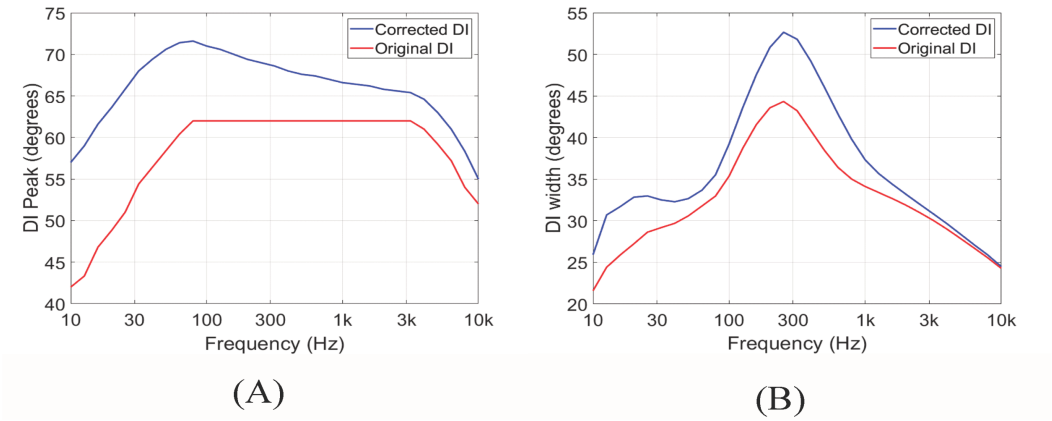

Figure 10: The angle of the peak directivity index as a function of frequency is shown in part (A) of the figure. Both the uncorrected and corrected curves are shown. Note that the peak directivity angle has moved upward to where it is experimenetally observed to be. Part (B) shows the width of the directivity peak, defined as the distance between the 3 dB down points of the directivity curves.

This second correction was possible because we had intensity data from a similar booster that allowed location of the sound source as a function of frequency more precisely than was possible before. Of course, that required the assumption that the scaling of the sound source position by nozzle diameter is the correct scaling. Using the new source location we were able to geometrically locate each microphone relative to the source both in angle and distance, and scale the SPL to a common distance (80 nozzle diameters) using spherical spreading.

These new directivity indices agree better with those measured in actual launches and static fires, and match better with the Mach wave radiation mechanism. We also see hints that 80 nozzle diameters may be far enough away that the high-frequency distribution is not characteristic of the source, but may be more influenced by nonlinear propagation and shockwave formation.

REFERENCES

[1] K. M. Eldred, "Acoustic loads generated by the propulsion system," NASA SP-8072, Washington, DC (1971).

[2] S. A. McInerny, J. K. Wikiser, R.H. Mellen, "Rocket Noise Propagation", In ASME International Mechanical Engineering Congress and Exposition Vol. 18480. American Society of Mechanical Engineers (1997).

[3] Logan T. Mathews, Kent L. Gee, Grant W. Hart "Characterization of Falcon 9 launch vehicle noise from far-field measurements" J. Acoust. Soc. Am. **150** 620-633 (2021).

[4] Grant W. Hart, Logan T. Mathews, Mark C. Anderson, J. Taggart Durrant, Michael S. Bassett, Samuel A. Olausson, Griffin Houston, and Kent L. Gee, "Methods and results of acoustical measurements made of a Delta IV Heavy launch", Proc. Mtgs. Acoust. **45**, 040003 (2021).

[5] R. Jeremy Kenny, Chris Hobbs, Ken Plotkin, and Debbie Pilkey "Measurement and Characterization of Space Shuttle Solid Rocket Motor Plume Acoustics", 15th AIAA/CEAS Aeroacoustics Conference (30th AIAA Aeroacoustics Conference) AIAA-2009-3161 (2009)

[6] Debbie Pilkey and Robert Jeremy Kenny, " A review of large solid Rocet Motor Free Field Acoustics, Part I", Presentation given at 162nd ASA meeting, San Diego, CA, Accessed from NASA Technical Reports Server, Document 20120001760 (2011).

[7] Jared Haynes and Robert Kenny "Modifications to the NASA SP-8072 Distributed Source Method II for Ares I Lift-Off Environment Predictions", 15th AIAA/CEAS Aeroacoustics Conference (30th AIAA Aeroacoustics Conference) AIAA-2009-3160 (2009)

[8] Michael M. James, Alexandria R. Salton, Kent L. Gee, Tracianne B. Neilsen, Sally A. McInerny, R. Jeremy Kenny "Modification of directivity curves for a rocket noise model", Proc. Mtgs. Acoust **18** 040008 (2012)

[9] Kent L. Gee, R. Jeremy Kenny, Tracianne B. Neilsen, Trevor W. Jerome, Christopher M. Hobbs and Michael M. James "Spectral and statistical analysis of noise from reusable solid rocket motors", Proc. Mtgs. Acoust. 18 040002 (2012)

[10] Kent L. Gee, Whiting, E. B. , Neilsen, T. B. , James, M. M. , and Salton, A. R. ''Development of a near-field intensity measurement capability for static rocket firings," Trans. JSASS Aerosp. Tech. Jpn. **14**, Po_2_9–Po_2_15 (2016).

[11] Caroline P. Lubert, Kent L. Gee, Seiji Tsutsumi "Supersonic jet noise from launch vehicles: 50 years since NASA SP-8072", J. Acoust. Soc. Am., **151**, 752-791 (2022).

[12] Mylan R. Cook, Kent L. Gee, Scott D. Sommerfeldt, "A coherence-based phase and amplitude gradient estimator method for calculating active acoustic intensity" J Acoust Soc Am 151, 4053–4060 (2022) https://doi.org/10.1121/10.0011731